

Numerical Back-Analysis of Structurally Controlled Cave Initiation and Propagation at the Henderson Mine

Sainsbury, D. P. and Sainsbury, B. L.

Itasca Australia, Melbourne, Victoria, Australia

Board, M. P.

Itasca Denver, Lakewood, Colorado, USA

Loring, D.M.

Climax Molybdenum, Empire, Colorado, USA

Copyright 2011 ARMA, American Rock Mechanics Association

This paper was prepared for presentation at the 45th US Rock Mechanics / Geomechanics Symposium held in San Francisco, CA, June 26–29, 2011.

This paper was selected for presentation at the symposium by an ARMA Technical Program Committee based on a technical and critical review of the paper by a minimum of two technical reviewers. The material, as presented, does not necessarily reflect any position of ARMA, its officers, or members. Electronic reproduction, distribution, or storage of any part of this paper for commercial purposes without the written consent of ARMA

ABSTRACT: A numerical approach to cave assessment has been developed over the past 12 years, partly through funding provided by the International Caving Study (ICS) and Mass Mining Technology (MMT) Projects. Recent improvements have been made to the modeling methodology that allows the explicit representation of large, persistent geological structures within a cave-scale model. A numerical back-analysis of structurally controlled cave initiation and propagation has been conducted at the Henderson Mine to provide a validation of the modeling methodology. Evolution of the numerically derived yield zone during cave initiation and propagation provides a good match to measured TDR (Time Domain Reflectometry) breakages surrounding the cave volume. Interaction of the propagating cave with a weak geologic contact was required to be captured within the numerical model in order to achieve this correspondence.

1. INTRODUCTION

Prediction of the initiation and propagation behavior of a block/panel cave has become increasingly more important in the past decade as mining in hard rock and coal have moved toward higher production, lower cost methods. Since the inception of cave mining methods in the iron ore mines of northern Michigan, USA, during the early part of the 20th century, researchers have sought to understand and predict the nature of cave propagation through simple one-dimensional volume-based relationships and empirical methods. Although these methods have been successfully applied to many cave operations to-date, numerical modeling is considered to be able to provide a more fundamental, rigorous and robust assessment of cave propagation behavior.

A numerical approach to cave assessment has been developed over the past 12 years during the industry funded International Caving Study (ICS I & II) and Mass Mining Technology (MMT) projects. Numerical algorithms are used to represent the primary mechanisms of undercutting, draw and cave propagation within the three-dimensional, continuum-based program FLAC3D [1].

The effect of large-scale geologic structures on caving and associated subsidence behavior has been recognized at many operating and abandoned cave mining operations. Recent improvements have been made to the modeling methodology that allows the explicit

representation large-scale geological structures. Back-analysis of structurally controlled cave initiation and propagation of the 7210 Level at the Henderson Mine provides validation of the modeling methodology.

2. THE HENDERSON MINE

Climax Molybdenum Company's Henderson Mine is an underground panel-caving mine located in Clear Creek County Colorado and is 9 miles west of Empire, Colorado, USA. Figure 1 provides a general cross-section of the mining geometry.

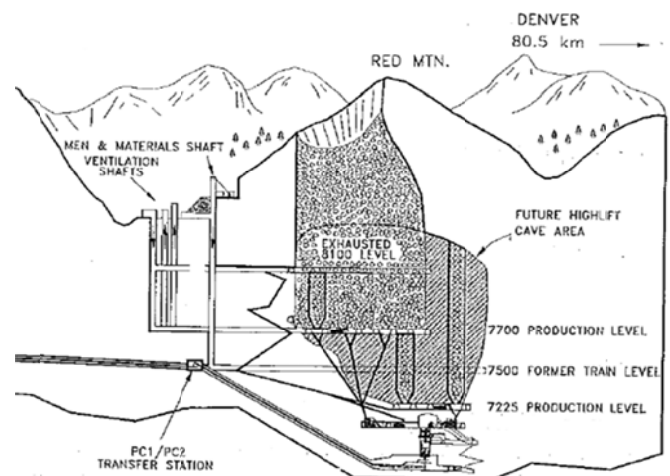


Fig. 1. Cross Section of the Henderson Mine [2]

Figure 2 illustrates a cross-section through the intrusive geological setting which comprises the Henderson orebody.

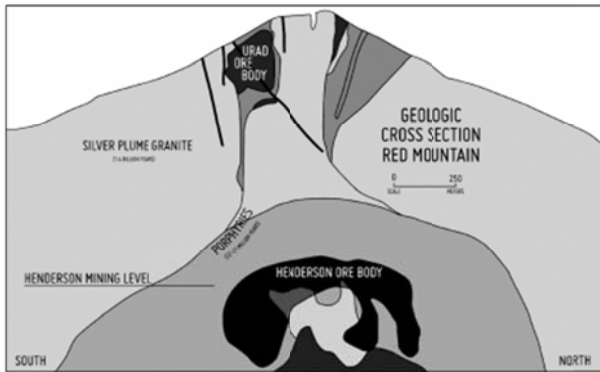


Fig 2 Schematic geologic cross-section

From 1976-1991, approximately 90 million tonnes of ore were produced from the 8100 level, while the 7700 level was brought into production during 1992. During initial development of the 7210 level in 2005, a weak intrusive contact was observed to effect the initiation, propagation and shape of the yielded rock mass zone.

3. NUMERICAL MODELING OF CAVING

The MMT-based numerical approach to cave assessment has successfully been employed in simulations of caving and subsidence response and validated at a number of different mines that include:

- Northparkes E26 Mine [3]
- Palabora Mine [4]
- Grace Mine [5]

The numerical algorithms used to represent the primary mechanisms of undercutting, draw, and cave propagation within FLAC3D and have previously been described in detail [4,6]. A bi-linear, Mohr-Coulomb, strain-softening constitutive model is used to simulate the rock mass and its progressive disintegration from a jointed rock mass to a caved material. Coupled with a production draw technique that accurately accounts for the mass balance of a dilating (bulking) rock mass, the numerical cave is allowed to evolve progressively upward from the undercut.

A conceptual model of caving has been developed [7]. The model includes four main behavioral regions - presented in Figure 3a. The characteristics of each region have been derived from in situ monitoring, underground observations and numerical simulations. They are defined below. Equivalent regions are determined within the numerical model during the caving simulation (Figure 3b).

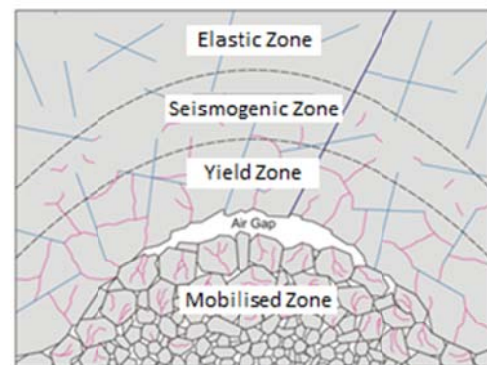
Elastic Region — The host rock mass around the caving region behaves mainly elastically and has properties consistent with an “undisturbed” rock mass.

Seismogenic Zone — Microseismic (and sometimes seismic) activity is concentrated in this region primarily due to slip along pre-existing discontinuities and the initiation of new fractures.

Yielded Zone — The rock mass in this region is fractured and has lost some or all of its cohesive strength. The rock mass within the yielded zone is subject to significant damage i.e., open holes are cut-off, TDRs break and cracking is observable in infrastructure. Stress components within this region are typically low in magnitude.

Mobilized Zone — This zone gives an estimate as to the portion of the orebody that has moved at least 1-2m in response to the production draw and may be recoverable.

a) Conceptual Model



b) Numerical Model of Caving

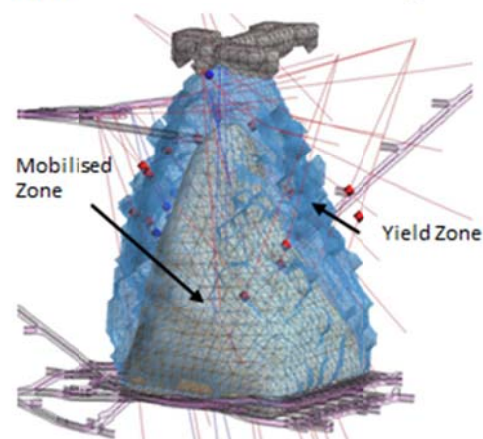


Fig. 3. a) Conceptual model of cave behavioural regions; b) Mobilised and Yield zones within numerical model of caving

4. EFFECT OF GEOLOGICAL STRUCTURES ON CAVING AND SUBSIDENCE BEHAVIOR

The influence of geologic structure on ground subsidence profiles and cave propagation rates/shape is

recognized to be important by many researchers [8,9,10,11,12,13,14,15,16,17,18,19,20,21,22].

In situ observations [8,12,13,23,24,25] have shown that the impact of structure can be varied based on persistence, strength and orientation relative to the mining footprint and principal stress direction. Quantifying the effects of large-scale structures is complicated by the fact that many features have not reacted adversely when subjected to subsidence and the results of scientific investigations are in some instances contradictory [21].

Previous studies [26,27] report that major structures can modify or enlarge a crater perimeter by further break back, and the presence of a steeply dipping fault can terminate the angle of draw short of its normal value, as illustrated in Figure 4. If a gently dipping fault intersects the collapsing rock column the lateral extent of surface subsidence can increase outward to the place where the fault intersects the ground surface.

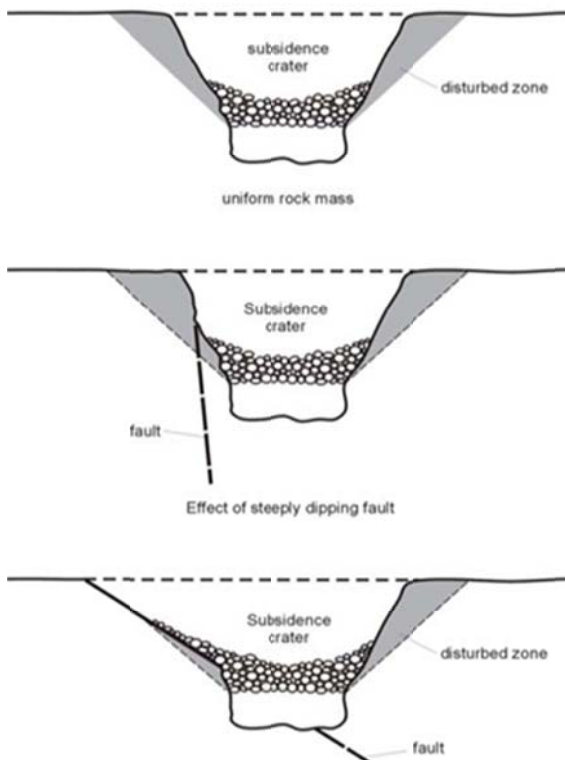


Fig. 4. Crater shape modified by major geological structure [27]

One of the first problems associated with analyzing the effects of geologic structure on ground movements is characterizing the structure properties. These properties are highly variable and include: orientation, infill material, previous displacement planarity and shear strength. They are historically difficult to determine either *in situ* or in the laboratory. However, whether or not a geological structure affects cave propagation and subsidence depends primarily on the shear strength of

the fault zone [28]. This fact has also been noted by other researchers.

5. NUMERICAL SIMULATION OF LARGE-SCALE GEOLOGICAL STRUCTURES

The FLAC3D code allows for the simulation of geological structures with either an implicit continuum-based approach termed “ubiquitous joints” or a discrete approach that uses an interface between separate numerical grids.

Interfaces have the properties of friction, cohesion, and dilation, and normal and shear stiffness, as illustrated in Figure 5a. Although there is no restriction on the number of interfaces or the complexity of their intersections, historically, interfaces have not been used to simulate geological structures due to difficulties in creating complicated geometries. However, recent advances in automated mesh generation have made it possible to create models with many irregular and intersecting interfaces, as illustrated in Figure 5b.

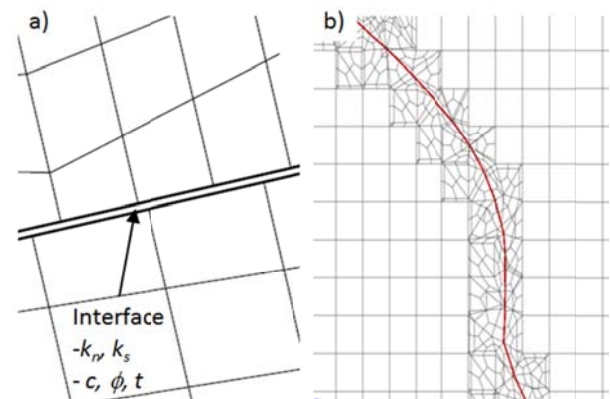


Fig. 5. a) Schematic of interface logic; b) cross-section through irregular interface in three-dimensions.

Several researchers have investigated the effect of large-scale structures on cave propagation and subsidence using two-dimensional modeling techniques. Such analyses do provide insight into the mechanisms of cave – structure interaction, however, there is concern that a plane strain approach can over-estimate the influence of major structures and is not well suited to studying the potential for a cave to stall - as it does not allow for the three-dimensional concentration of stresses in the cave back.

To investigate the effect of geological structure on cave behavior, a simplified conceptual block cave mine has been simulated. The mining footprint has dimensions of 120 m x 120 m (Hydraulic Radius (HR) of 30) and is located at a depth of 600 m below the ground surface. The maximum principal horizontal stress has been simulated at twice the vertical stress. Production has been simulated as a total height of draw (HOD) of 10 m as illustrated in Figure 6. A detailed sensitivity study

using the same conceptual model to investigate the effect of rock mass strength, brittleness (softening), *in situ* stress and draw strategy on cave propagation has been completed [29].

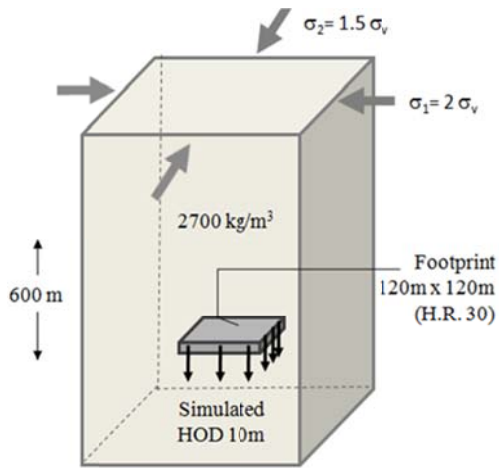


Fig. 6. Conceptual cave model

The geomechanical properties used to simulate the rock mass within the conceptual cave model are presented in Table 1. Segments 1 and 2 refer to the bi-linear segments of a linear approximation to the Hoek-Brown failure envelope.

Table 1. Rock mass geomechanical properties

σ_c (MPa)	GSI	m_i	E_m (GPa)	ν_m	Segment 1		Segment 2		Tens. (MPa)
					Coh. (MPa)	ϕ (Deg.)	Coh. (MPa)	ϕ (Deg.)	
120	55	14	13.3	0.3	2.2	52	6.8	38	0.3

In order to study the effects of geological structures on cave propagation behavior and validate the modeling methodology, a series of idealized structures were introduced to the conceptual cave model. Figure 7 illustrates the orientation of the five structures simulated.

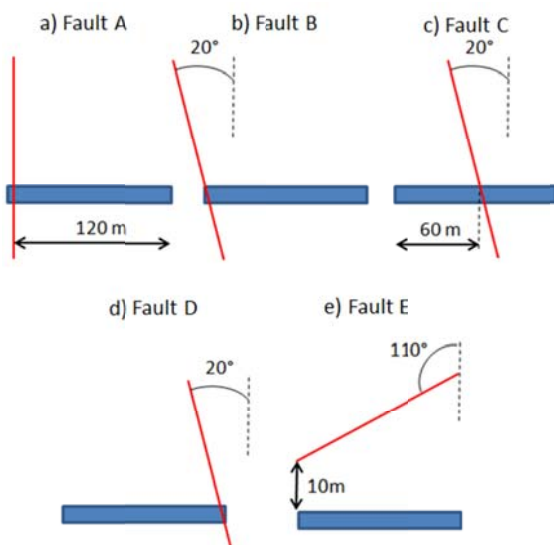


Fig. 7. Conceptual geological structures simulated

Three property sets, presented in Table 2, were derived to provide a representative upper, average and lower bound range of the stiffness, shear and tensile strength of large-scale geological structures.

Table 2. Fault stiffness, shear and tensile strengths simulated

Set	K_n (GPa/m)	K_s (GPa/m)	Coh. (kPa)	ϕ (Deg.)	Tens. (MPa)
1	1	0.1	0	20	0
2	10	1	75	30	0
3	50	5	100	40	0

Figure 8 illustrates the mobilized and yield zones of different conceptual models with Set 2 strengths. The presence of the fault is observed to affect the propagation rate and shape of the cave.

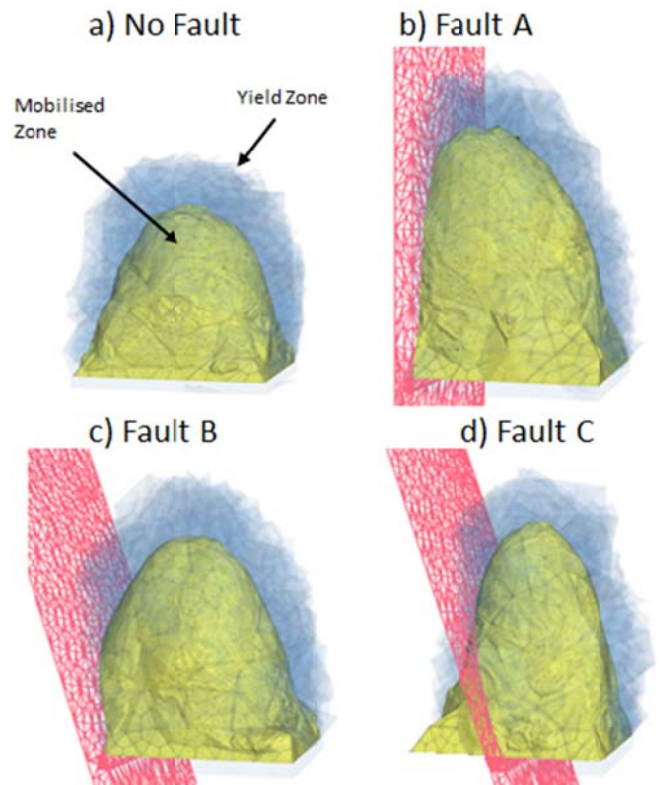


Fig. 8. Simulated mobilized and yield zones after 10m height of draw.

Figure 9 illustrates a cross-section of the mobilized (caved) zone through the center of the conceptual model. The effect of increasing fault strength and stiffness is clearly observed. The weak vertical structure (Figure 9a) causes an increased cave propagation rate. The vertical sub-vertical structures (Fault B, C and D) all display some effect on the shape of the mobilized zone. The sub-horizontal structure (Fault E) displays only a very minor effect on the shape of the mobilized zone.

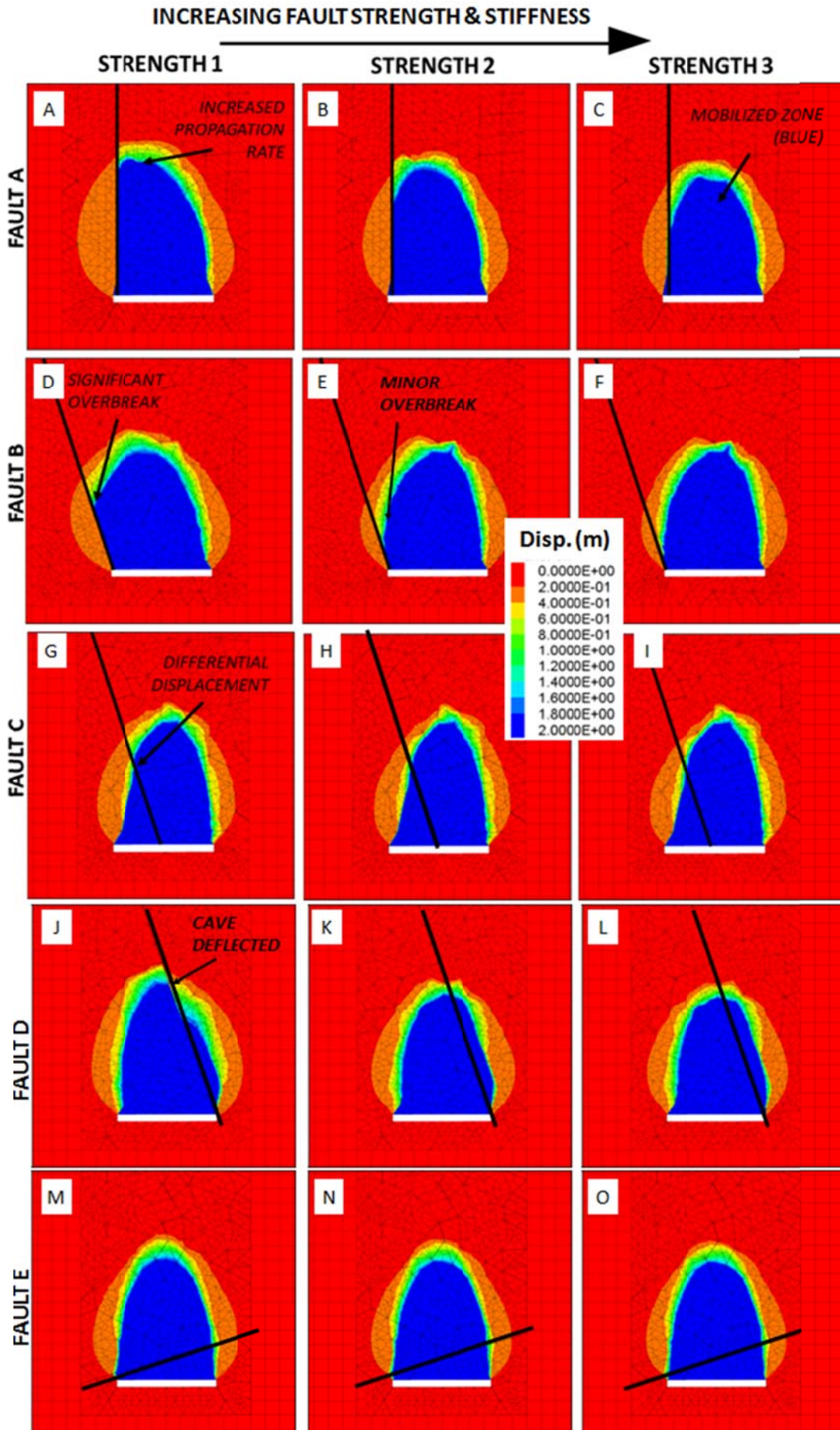


Fig. 9. Cross-section of mobilized zone (mobilized zone given by 2m displacement contour)

Although the results of the conceptual models are generally qualitative in nature, the mobilized zones are consistent with the trends reported throughout the literature (Figure 4).

6. BACK-ANALYSIS OF STRUCTURALLY CONTROLLED CAVE INITIATION AND PROPAGATION AT THE 7210 LEVEL

6.1. Background

A weak geological contact has been observed to effect cave propagation and cave shape on the 7210 Level at the Henderson Mine. During undercutting of the 7210 Level in 2005, cave initiation was observed with a relatively small undercut hydraulic radius (22 m) compared to what has been observed during other cave initiations at the Mine (35 m). The presence of intrusive contacts along the northern boundary of the 7210 Level undercut has previously been reported as being responsible for premature cave initiation [30] (Figure 10a). Past experience at the Henderson confirms this.

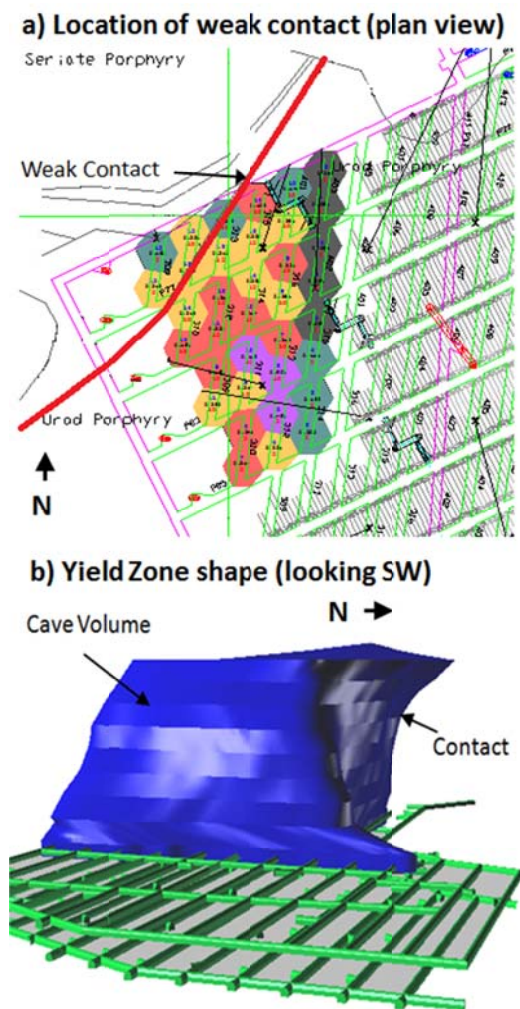


Fig. 10. a) Plan view of weak contact; b) 7210 Level yield zone during December 2007

During early August 2006, migration of the propagating cave beyond the undercut footprint on the north and west sides was observed along the weak intrusive contact. Figure 10b illustrates the shape of the 7210 Level yield zone during December 2007 as defined by TDR breaks.

6.2. Model Geometry and Production Schedule

A large-scale FLAC3D model was constructed to simulate the regional extents of the Henderson Mine, as illustrated in 11a. The existing cave volumes (8100 and 7700), developed prior to the 7210 Level were initialized within the model based upon historical mining records, as illustrated in 11b.

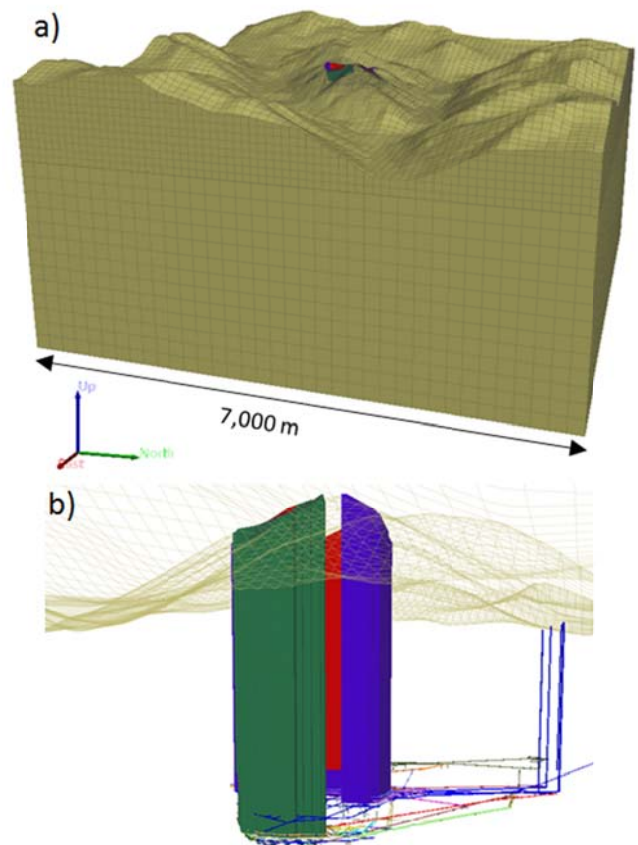


Fig. 11. a) Regional extents of model; b) existing cave volumes

The weak contact between the Seriate and Urad Porphyry was simulated with an interface element in FLAC3D as illustrated in Figure 12.

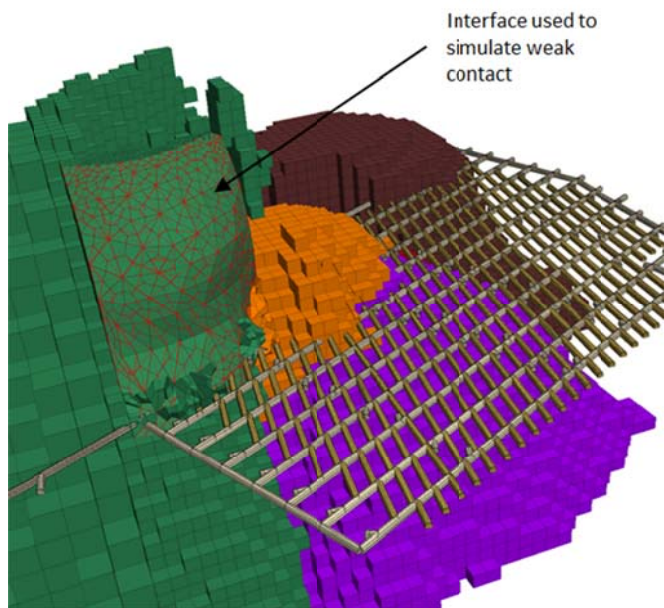


Fig. 12. Interface used to simulate weak contact

The evolution of draw height simulated within the model (based upon the actual production records) is illustrated in Figure 13.

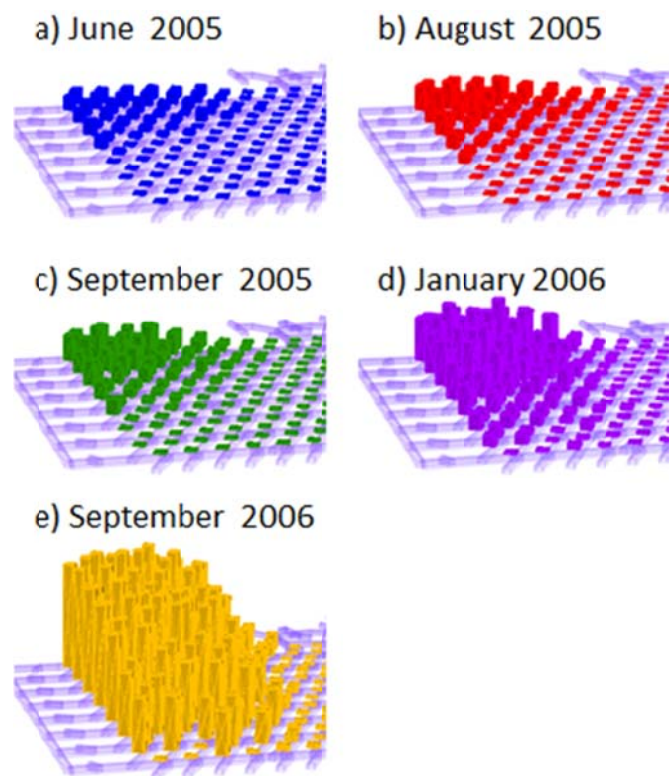


Fig. 13 Simulated production schedule (cumulative solid rock height of draw) based on actual draw heights

6.3. Material Properties and Pre-Mining Stresses

Multiple geotechnical domains have been mapped throughout the 7210 Level. The geomechanical properties used to simulate the main caving domain, the Urad Porphyry, are presented in Table 3.

Table 3. Rock mass geomechanical properties

σ_c (MPa)	GSI	m_i	E_{rm} (GPa)	ν_{rm}	Segment 1		Segment 2		Tens. (MPa)
					Coh. (MPa)	ϕ (Deg.)	Coh. (MPa)	ϕ (Deg.)	
118	55	10	11	0.2	2.3	48	6.3	35	0.4

Table 4 presents the interface material properties used to simulate the weak geological contact.

Table 4. Interface geomechanical properties

Set	Kn (GPa/m)	Ks (GPa/m)	Coh. (kPa)	ϕ (Deg.)	Tens. (MPa)
1	1	0.1	0	20	0

Due to the significant topographic relief and complex previous mining history at Henderson, it is difficult to estimate the pre-mining stress regime. A stress calibration exercise has previously been conducted at Henderson [31], whereby nine stress measurements taken from 1970 to 1989 were calibrated determining the in situ tectonic stresses that result in a best-fit of model predicted stress to those measured by overcoring. The results of the stress calibration exercise, which indicated a major principal stress oriented at 155 degrees, were directly applied to the back-analysis model.

6.4. Model Results

The evolution of the model-predicted yield zone is illustrated in Figure 14. The modeled yield zone is observed to provide a close match to the TDR breakages (blue spheres) monitored during cave propagation. Shear failure along the weak contact can be observed to develop along the interface - coincident with vertical propagation of the yield zone. After initial breakthrough of the yield zone to the overlying 7700 Level in January 2006, the yield zone is observed to follow the weak contact outside the northern and western limits of the undercut footprint. The modeled cave breakthrough timing and dimensions match closely the observed 7700 level breakthroughs as shown Figure 14.

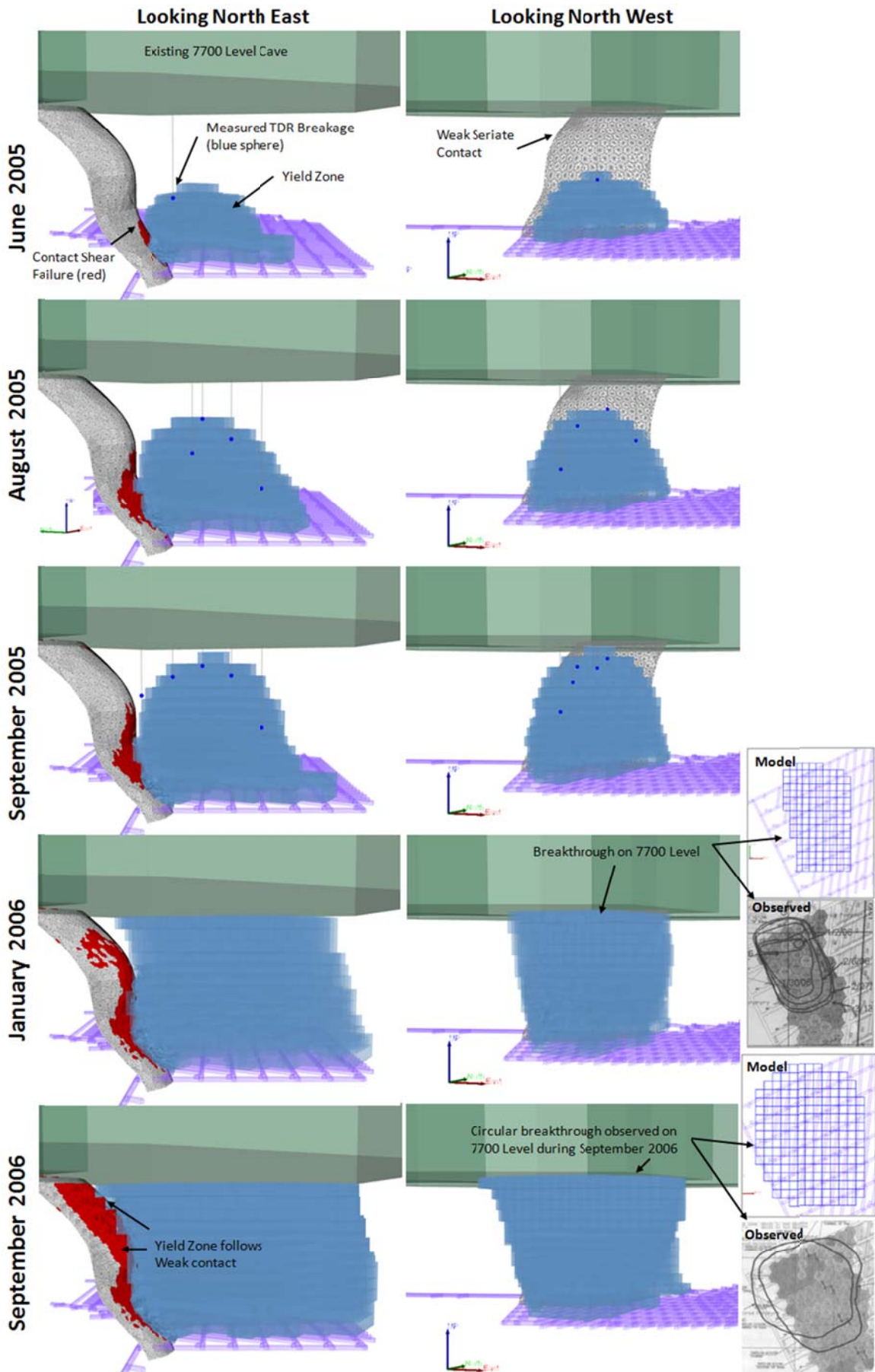


Fig. 14. Evolution of cave yield zone

Figure 15 illustrates a comparison between the shape modeled and actual yield zones after September 2006. The model provides a close match to the actual observed conditions.

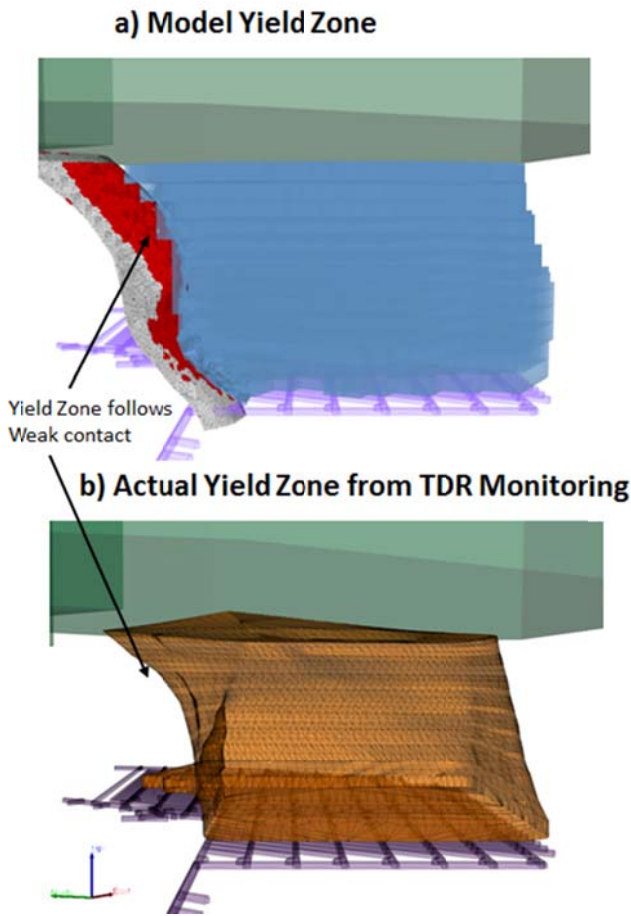


Fig. 15. Comparison of modeled versus actual cave shape

6.5. Effect of the Weak Structure on Cave Initiation

In order to demonstrate the effect of the weak contact on cave initiation, an analysis was conducted without the structure. As illustrated in Figure 16, the yield zone height is significantly impacted by the weak interface with height reduced by approximately 30 m at the June 2005 state. Clearly, the cave shape and growth and the ability to predict this behavior depends on the presence of the weak interface.

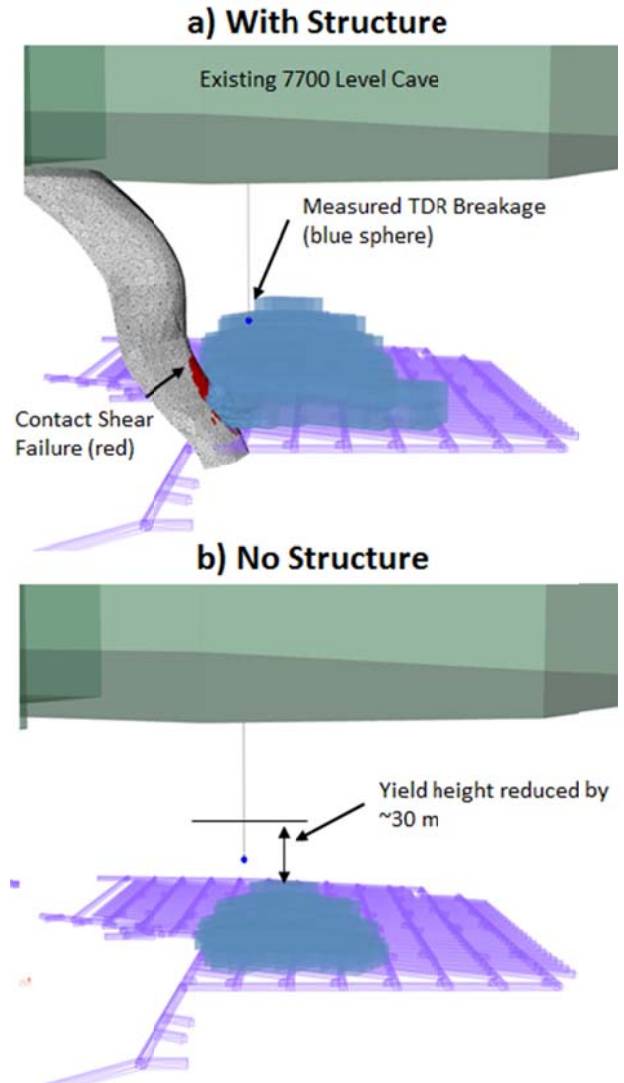


Fig. 16. Comparison of cave initiation with and without a weak structure

7. SUMMARY AND CONCLUSIONS

Back-analysis of cave behavior at the 7210 Level of the Henderson Mine provides a close match to the observed and monitored yield zone propagation rate and shape. The analysis validates the MMT-based numerical model of caving and the simulation of weak geological structures with interfaces elements in FLAC3D.

8. ACKNOWLEDGEMENTS

The authors would like to thank the management of Climax Molybdenum and the Henderson Mine for the permission to publish this work.

REFERENCES

1. Itasca Consulting Group, Inc. 2009. FLAC3D – Fast Lagrangian Analysis of Continua in 3 Dimensions, Ver. 4.0, User's Manual. Minneapolis: Itasca.
2. Rech, W.D. 2001. Underground Mining Methods. Engineering Fundamentals and International Case Studies, Chapter 48 - Henderson Mine. Hustrulid, W. and R. Bullock (eds). Society for Mining and Exploration.
3. Pierce, M., Cundall, P. Mas Ivars, D., Darcel, C., Young, R.P., Reyes-Montes, J. & Pettitt, W. 2006a. Six Monthly Technical Report, Caving Mechanics, Sub-Project No. 4.2: Research and Methodology Improvement, & Sub-Project 4.3, Case Study Application, Itasca Consulting Group Inc, Report to Mass Mining Technology Project, 2004-2007, ICG06-2292-1-Tasks 2-3-14, March.
4. Sainsbury, B., Pierce, M. & Mas Ivars, D. 2008. Analysis of Caving Behavior Using a Synthetic Rock Mass —Ubiquitous Joint Rock Mass Modeling Technique, In Proceedings of the 1st Southern Hemisphere International Rock Mechanics Symposium (SHIRMS), Y. Potvin, J. Carter, A. Dyskin and R. Jeffrey (eds), 16–19 September 2009, Perth, Australia, Australian Centre for Geomechanics, Perth, Vol. 1 – Mining and Civil, pp. 243–254.
5. Sainsbury, D., Lorig, L. and Sainsbury, B. 2010. Investigation of caving induced subsidence at the abandoned Grace Mine, in Caving 2010: Second International Symposium on Block and Sublevel Caving. 20–22 April 2010, Australian Centre for Geomechanics.
6. Board, M. and Pierce, M. 2009. A review of recent experience in modeling of caving, International Workshop on Numerical Modeling for Underground Mine Excavation Design June 28, 2009 Asheville, North Carolina in Conjunction with the 43rd U.S. Rock Mechanics Symposium.
7. Duplancic, P. and Brady, B.H. 1999. Characterization of caving mechanisms by analysis of seismicity and rock stress, Proceedings 9th International Congress on Rock Mechanics (Paris, 1999), Balkema: Rotterdam, Vol. 2, pp. 1049–1053.
8. Crane W.R. 1929. Subsidence and Ground Movement the Copper and Iron Mines of the Upper Peninsula, Michigan. USBM Bulletin 285, 66 pp.
9. Crane W.R. 1931. Essential Factors Influencing Subsidence and Ground Movement, USBM IC 6501 14 p.
10. Heslop T.G. 1974. Failure by Overturning in Ground Adjacent to Cave Mining at Havelock Mine, 3rd. ISRM Congress, Denver.
11. Boyum, B H, 1961. Subsidence case histories in Michigan mines. Proceedings 4th Symposium on Rock Mechanics, Bulletin, Mineral Industries Experiment Station, Pennsylvania State University, No 76: 19-57
12. Fletcher J.B. 1960. Ground Movement and Subsidence from Block Caving at Miami Mine, AIME Transactions, v. 217, pp 413-421.
13. Parker J. 1978. What Can Be Learned From Surface Subsidence, E&MJ, July 1978.
14. Laubscher, D. 1990. A geomechanical classification system for the rating of rock mass in mine design. Journal of the South African Institute of Mining and Metallurgy. Vol. 90, No. 10, pp. 257-273.
15. Mahtab M. 1976. Influence of Rock Fractures on Caving, Trans. AIME, Vol 260.
16. Hoek, E. 1974. Progressive caving induced by mining an inclined orebody. Trans Instn Min Metall, Sect A: Min Industry, 83: A133-139.
17. Peng S.S. 1992. Surface Subsidence Engineering, Society For Mining, Metallurgy and Exploration Inc., Littleton, Colorado. 161 pp.
18. Holla L. and Buizen M. 1990. Strata Movement Due to Shallow Longwall Mining and the Effect on Ground Permeability. Proc. Aus. IMM, No. 1, pp 11-18.
19. Shadbolt C.H. 1978. Mining Subsidence - Historical Review and State of the Art, Conf. on Large Ground Movements and Structures, Cardiff. Pantech Press, London, ed. J.D. Geddes. pp 705-748.
20. Shadbolt C.H. 1987 A Study of the Effects of Geology On Mining Subsidence in the East Pennine Coalfield. Ph.D. Thesis, University of Nottingham.
21. Hellewell F.G. 1988. The Influence of Faulting on Ground Movement due to Coal Mining: The U.K. and European Experience. Mining Engineer, 147, pp 334-337.
22. Vyazmensky A., Elmo, D. and Stead, D. 2010. Role of Rock Mass Fabric and Faulting in the Development of Block Caving Induced Surface Subsidence, Rock Mech. Rock Eng 43:533–556.
23. van As, A, Davison, J. and Moss, I. 2003. Subsidence Definitions for Block Caving Mines. Rio Tinto Technical report. 59pp.
24. Blodgett, S. and Kuipers, J. 2002. Underground Hard-Rock Mining: Subsidence and Hydrologic Environmental Impacts, Centre for Science in Public Participation.
25. Hatheway, A.W. 1966. Engineering geology of subsidence at San Manuel mine, Pinal County, Arizona: M.S. thesis, University of Arizona, Tucson, 110 pp.
26. Butcher, R. 2005. Subsidence effects associated with block and sublevel caving of massive orebodies, Australian Centre for Geomechanics Newsletter, Volume No. 25
27. Stacey, T.R. & Swart, A.H. 2001. Practical rock engineering practice for practice for shallow and opencast mines. SIMRAC The safety of mines research advisory committee, 66pp.

28. Abel, J.F. and Lee, F.T. 1980. Subsidence Potential in Shale and Crystalline Rocks, USGS, OFR 80-1072.
29. Sainsbury, B. 2010. Sensitivities in the numerical assessment of cave propagation in Caving 2010: Second International Symposium on Block and Sublevel Caving. 20–22 April 2010, Australian Centre for Geomechanics.
30. Carlson, G., and R. Golden Jr. 2008 Initiation, Growth, Monitoring and Management of the 7210 Cave at Henderson Mine --- A Case Study, in MASSMIN 2008 (5th International Conference on Mass Mining, Luleå, Sweden, June 2008), pp. 97-106, H. Schunnesson and E. Nordlund, Eds. Luleå: Division of Mining & Geotechnical Engineering, Luleå University of Technology.
31. Rech, W.D. and L. Lorig. 1992. Predictive numerical stress analysis of panel caving at the Henderson Mine. MASSMIN '92. Johannesburg, SAIMM, pp. 55-62.